Thermodynamics of ion exchange coupled with swelling reactions in hydrated clay minerals

Subramanian, Nithya; Nielsen Lammers, Laura

DOI
10.1016/j.jcis.2021.09.106

Publication date
2022

Document Version
Final published version

Published in
Journal of Colloid and Interface Science

Journal of Colloid and Interface Science 608 (2022) 692–701

Contents lists available at ScienceDirect

Journal of Colloid and Interface Science

journal homepage: www.elsevier.com/locate/jcis

Thermodynamics of ion exchange coupled with swelling reactions in hydrated clay minerals

Nithya Subramanian [a,*], Laura Nielsen Lammers [b,c]

[a] Faculty of Aerospace Engineering, Technische Universiteit Delft, Zuid Holland, the Netherlands
[b] Department of Environmental Science, Policy, and Management, University of California Berkeley, CA, USA
[c] Earth and Environmental Sciences Area, Lawrence Berkeley National Laboratory, CA, USA

GRAPHICAL ABSTRACT

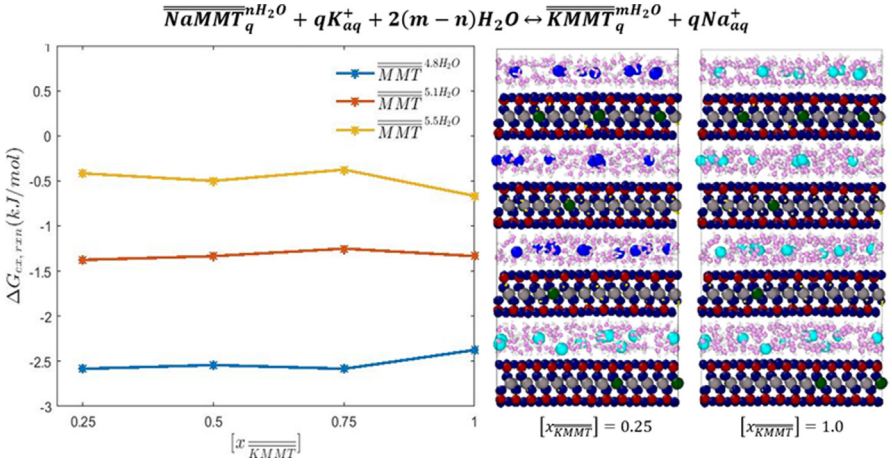

ARTICLE INFO

Article history:
Received 3 July 2021
Revised 17 September 2021
Accepted 19 September 2021
Available online 27 September 2021

Keywords:
Montmorillonite
Cation exchange
Thermodynamics
Swelling
Solution chemistry

ABSTRACT

Crystalline hydrates of swelling clay minerals (smectites) exhibit a strong coupling between their ion exchange and hydration/dehydration reactions. The uptake or removal of water from smectite interlayers as a result of a change in the environmental conditions also leads to the partitioning of cations. Three factors, the solid ion composition, the solid basal spacing/water content, and the aqueous solution composition, are all implicated in controlling the thermodynamics of ion exchange. However, conventional approaches to measuring the exchange free energy cannot separate the influence of each of these individual factors. Here, we explore the energetics of the swelling and ion exchange reactions in montmorillonite using a potential of mean force approach and the thermodynamic integration method within molecular simulations. We investigate the influence of solution and clay composition on the spontaneity of the reactions, focusing on the 2 water-layer hydration state. The swelling simulations provide the equilibrium water content, interlayer water structure, and basal spacings, while thermodynamic integration of sodium–potassium exchange in the aqueous solution and solid phase are combined to calculate ion exchange free energies as a function of solution composition. Results confirm the tendency of the clay to collapse to lower hydration states as the concentration of the solution increases. Changes to the equilibrium water content, even at fixed hydration states, and the composition of the mixed electrolyte solution play a critical role in driving ion exchange and the selectivities of the clay to the exchanged cation,

* Corresponding author.
E-mail address: n.subramanian-1@tudelft.nl (N. Subramanian).

https://doi.org/10.1016/j.jcis.2021.09.106

while the composition of the solid phase is shown to be insignificant. These findings underscore the extreme sensitivity of clay swelling and ion exchange thermodynamics to small (tenths of an Angstrom) deviations in layer spacing.

1. Introduction

The adsorption/desorption of micronutrients and the accumulation/dilution of industrial contaminants in soils that eventually impact the health and safety of the biosphere are controlled by ion exchange processes. Ion exchange processes are also extensively used for the selective removal of heavy metals from wastewater, water softening, and the recovery of Li^+, Na^+, etc. from geologic resources and from spent metal ion batteries. Due to its wide-ranging applications, ion exchange is considered the second most important reaction on earth following photosynthesis [1]. Exchangers that enable the transfer of ions could be engineered membranes (with targeted selectivities) [2], polymeric resins [3], or natural materials such as zeolites [4] and clays.

Clays, particularly smectites (swelling clays), which are critical components of engineered geological barriers for the safe, long-term storage of nuclear waste, exhibit high cation exchange capacity (CEC). Montmorillonites (MMT – a type of smectite clay mineral) are effective barriers because their expansive behavior, upon contact with water, fills the voids between the container and the wall rock providing sufficient sealing of the nuclear waste repository. Furthermore, the intrinsic negative charge on the MMT layers mitigates the diffusion and transport of radionuclides that tend to form oxyanions [5]. It is well established that montmorillonite clays adopt crystalline hydration states, with defined water contents [6–9] (1-, 2- and 3- water layer states). In geological waste repositories, the dominant hydration content in the clay-rich barrier correspond to the 2- (2 W) and 3-water layer (3 W) swelling states. Numerous physical and chemical variables have a major influence on swelling states such as water activity [10], cation composition [8,11,12], and confining pressure[13,14]. Additionally, the type and composition of cation in the interlayer determines the equilibrium water content and basal spacing for a specific hydration state [8,15].

Due to their high CEC, swell/shrink reactions and ion exchange processes in smectites are tightly coupled. Interlayers of different hydration states are distinct phases that exhibit unique selectivities of adsorption for alkali metal cations. Li & Schultess [16] modeled competitive ion exchange in saturated MMT in the crystalline regime, among isovalent cations by curve-fitting X-ray diffraction data using model parameters from first-principles density functional theory and *a priori* knowledge of the clay composition. They confirmed that the exchange of Cs^+ with NaMMT was accompanied by a collapse of the interlayer region and observed the broadening and presence of multiple basal spacing peaks suggesting that in the case of incomplete ion exchange, the interlayers are segregated with unique cations. Recently, a comprehensive study [17] addressed critical questions pertaining to the coupling between swelling states and ion exchange in montmorillonite. The authors predicted stable equilibrium hydration states as a function of water and ion activities in solution and the cationic partition in clay when aqueous activity conditions are changed in a dynamic environment. Furthermore, Whittaker et al. [18] showed that an ion exchange driven change in water content (swelling state) is often associated with a restructuring of the interlayer depending on the cation that is exchanged into the clay phase. Evidence thus suggests that the ion exchange can drive the swelling or collapse of interlayers in smectites, and that the hydration and ion exchange reaction energetics are coupled. Understanding this coupling is critical to model the feedbacks arising from changes to microstructure and chemical composition that eventually control diffusion and transport in nuclear waste barriers.

Studies spanning several decades have established that the selectivity of bulk swelling clays (i.e. mixtures of swelling states) follows the lyotropic series for alkali metal ions [19–21]. The interaction between the cation and the mineral basal surface/edges (depending on the pH) as well as the relative tendencies of the cations to be hydrated in the mineral interlayers were considered to be factors determining the order of selectivity. A paradigm shifting study on the ion exchange selectivity of clay minerals argued that exchange among isovalent cations is controlled by the selectivity of the solution phase for the strongly hydrated cation (the one with lower hydration enthalpy) rather than by clay particle surface selectivity [22]. The weakly hydrated cation, thus, tends to partition into the solid phase, while the other cation remains in the aqueous phase. Rotenberg et al. supported this conclusion with microcalorimetry measurements and molecular dynamics simulations to explain that the preferential adsorption of Cs^+ over Na^+ in montmorillonite is driven by the relative 'hydrophobicity' of Cs^+ compared to Na^+ in solution, and not its affinity for clay mineral surfaces [23]. While this shift in understanding explains the progressive clay selectivity for alkaline ions according to a balance between hydration and adsorption free energies, the influence of the aqueous phase composition (and concentration) on the selectivities has not been explored sufficiently. The two studies referenced above consider saturated clay minerals in dilute suspension (water activity,a_w 1) and computations of the free energy of exchange in the aqueous phase are performed based on a trace exchange of the cation without the presence of the anion. Therefore, the effect of aqueous ion pairing interactions [24] on the exchange free energy is neglected.

Cs^+ sorption on smectites, investigated in the presence of competing cations (Na^+, K^+, Ca^{2+}), highlighted a strong dependence of adsorption selectivity on ionic strength. This study emphasized the importance of accounting for competition from even trace ions in solution [25]. When multiple types of adsorption sites exist in the clay mineral (surface and edge sites, for example), the selectivity of a particular adsorption site can be enhanced or diminished as a function of electrolyte concentration [26]. Additionally, a study that computed the free energy of exchange between Na^+ and NH_4^+ in solution as a function of the mole fraction of NH_4^+ in the mixed electrolyte revealed a significant dependence of the exchange free energy on the solution composition [4]. Since it is established now that the state of hydration of cations in solution drives the favorability of exchange, there is a need to investigate how the energetics of ion exchange are altered in the presence of concentrated and mixed electrolytes in which the hydration shells of the cations may not be fully occupied [27–29].

Here, we address key questions that dictate the response of clay swelling and sorption behavior to changes in aqueous solution chemistry: (i) what effect does electrolyte composition (relative ion activities) exert on the spontaneity of ion exchange? (ii) how can we account for as well as isolate contributions from transition between swelling states and the deviations from equilibrium water content within the same swelling state in montmorillonite during ion exchange at a given water activity?

2. Methodology

2.1. Theory

In this study, the term 'swelling state' corresponds to an equilibrium 2 W or 3 W hydration state and a change to the swelling state corresponds to the transition between them. The overall swelling reaction, resulting in a change to the swelling state, for a pure end-member MMT can be written as follows, with equilibrium water content per layer of water per unit cell of clay for NaMMT and KMMT represented by *n* and *m*, respectively.

$$NaMMT_{2W} + nH_2O \leftrightarrow NaMMT_{3W} \tag{1}$$

$$KMMT_{2W} + mH_2O \leftrightarrow KMMT_{3W} \tag{2}$$

The overall ion exchange reaction for a fixed swelling state (2 W represented by double overbar, for instance) can be written,

$$\bar{\bar{NaMMT}}_q^{nH_2O} + qK^+_{aq} + 2(m-n)H_2O \rightarrow \bar{\bar{KMMT}}_q^{mH_2O} + qNa^+_{aq} \tag{3}$$

In this reaction, the change in water content *(m-n)* from the exchange reaction contains a factor of *2* owing to the ion exchange taking place at a fixed 2 W swelling state. Equilibrium is achieved when the chemical potentials of thermodynamic components in MMT and the solution are equal at a given composition.

As the reaction proceeds, the degree of exchange varies from 0 (exchange of traces of K^+ in a $\bar{\bar{NaMMT}}$) to 1 (complete exchange from homoionic $\bar{\bar{NaMMT}}$ to homoionic $\bar{\bar{KMMT}}$). In order to define reaction quantities, it is necessary to carefully set up the initial and final reference states and ensure that mass (including water) is conserved during the exchange reaction. In our definition of states, the number of water molecules in the clay ion exchange end-members is not equal. Therefore, for the solid phase ion exchange, we consider two sets of initial and final reference states with *n* and *m* water molecules per layer of water per clay unit cell, respectively. The overall exchange free energies are expressed as a function of the water and ion activities in solution as well as the water content per water layer in the clay interlayers (*m, n*). The reference state of the solution follows the conventional definition of the chemical potential of pure, non-interacting ions at 1.0 M concentration, and the activity coefficients for isovalent dissimilar ions are not assumed to be equal.

The overall reaction for ion exchange in a fixed swelling state (Eq. (3) for 2 W) can be broken up into three parts: the exchange in the aqueous phase, the exchange in the solid/clay phase, and the hydration/dehydration reaction resulting in a change in the equilibrium water content.

$$K^+_{aq} \rightarrow Na^+_{aq}(\text{aqueous phase}) \tag{4}$$

$$\bar{\bar{NaMMT}}_q^{nH_2O} \rightarrow \bar{\bar{KMMT}}_q^{nH_2O} \ (\text{solid phase}) \tag{5}$$

$$\bar{\bar{KMMT}}_q^{nH_2O} + 2(m-n)H_2O \rightarrow \bar{\bar{KMMT}}_q^{mH_2O} \ (\text{deviation from equilibrium water content}) \tag{6}$$

The Gibbs free energy for the overall reaction can be decomposed into its three contributions with $\Delta G_{ex,aq}$ and $\Delta G_{ex,\bar{\bar{MMT}}}$ representing the exchange free energies in the aqueous and solid phases, respectively. $\Delta G_{hyd,\bar{\bar{MMT}}}$ corresponds to the free energy change from the change in equilibrium water content between stable end-members of the exchange reaction (Eq. (6)). We assume here that the free energy change pertaining to the deviation in water content at a fixed swelling state is equal for the K^+ and Na^+ end-members (i.e., the free energy change for reaction (6) is assumed equal for $\bar{\bar{KMMT}}$ and $\bar{\bar{NaMMT}}$).

$$\Delta G_{ex,rxn} = \Delta G_{ex,aq} + \Delta G_{hyd,\bar{\bar{MMT}}} + \Delta G_{ex,\bar{\bar{MMT}}} \tag{7}$$

The Gibbs free energy of exchange in the aqueous phase is computed as a function of the ratio of ion activity coefficients in a mixed electrolyte.

$$\Delta G_{ex,aq} = \Delta G_{K\rightarrow Na,aq} = (\mu_{Na^+} - \mu_{K^+})$$

$$\mu_{Na^+} = \mu^0_{Na^+} + RTln(\gamma_{Na^+}(1-x_{K^+})); \mu_{K^+} = \mu^0_{K^+} + RTln(\gamma_{K^+}x_{K^+})$$

$$\Delta G_{ex,aq} = \Delta G_{K\rightarrow Na,aq} = \left[(\mu^0_{Na^+} - \mu^0_{K^+}) + RTln\frac{\gamma_{Na^+}}{\gamma_{K^+}} + RTln\frac{1-x_{K^+}}{x_{K^+}}\right] \tag{8}$$

Ion exchange calculations in the solid phase are realized through two ion exchange reactions at fixed water contents:

$$IE1: \bar{\bar{NaMMT}}_q^{nH_2O} + qK^+_{aq} \rightarrow \bar{\bar{KMMT}}_q^{nH_2O} + qNa^+_{aq} \tag{9a}$$

$$IE2: \bar{\bar{NaMMT}}_q^{mH_2O} + qK^+_{aq} \rightarrow \bar{\bar{KMMT}}_q^{mH_2O} + qNa^+_{aq} \tag{9b}$$

The corresponding free energies of these two reactions are written in terms of clay end-member free energies of formation in a dilute suspension $\left(G^f_{\infty H_2O}\right)$ and the immersion free energy of clay in aqueous solution $\left(G^i_{aq}\right)$.

$$\Delta G_{IE1} = \left(G^f_{\bar{\bar{KMMT}},nH_2O} - G^f_{\bar{\bar{NaMMT}},nH_2O}\right) + q\Delta G_{ex,aq} \tag{10a}$$

$$\Delta G_{IE2} = \left(G^f_{\bar{\bar{KMMT}},mH_2O} - G^f_{\bar{\bar{NaMMT}},mH_2O}\right) + q\Delta G_{ex,aq} \tag{10b}$$

Where $\left(G^f_{\bar{\bar{KMMT}},nH_2O} - G^f_{\bar{\bar{NaMMT}},nH_2O}\right)$ is the free energy of exchange in the solid phase $\left(\Delta G_{ex,\bar{\bar{MMT}}}\right)$ in Equation (7).

$$G^f_{\bar{\bar{NaMMT}},nH_2O} = G^f_{NaMMT,\infty H_2O} - G^i_{NaMMT,aq} \tag{11a}$$

$$G^f_{\bar{\bar{NaMMT}},mH_2O} = G^f_{NaMMT,\infty H_2O} - \left(G^i_{NaMMT,aq} + G^{\Delta hyd}_{NaMMT,aq}\right) \tag{11b}$$

Note that in Reaction (11b), there is an extra component $\left(G^{\Delta hyd}_{aq}\right)$ to the free energy of formation of an ion exchange end-member in an aqueous solution whose water content deviates from its equilibrium value (as described in Reaction (6)). Substituting Equations (11a) & b in equations (10a) & b, we get:

$$\Delta G_{IE2} - \Delta G_{IE1} = \left(G^{\Delta hyd}_{NaMMT,aq} + G^{\Delta hyd}_{KMMT,aq}\right) = 2\Delta G_{hyd,\bar{\bar{MMT}}} \tag{12}$$

As mentioned before, the influence of hydration/dehydration at a fixed swelling state is assumed equal for the $\bar{\bar{NaMMT}}$ and $\bar{\bar{KMMT}}$ end-members. Therefore, the contribution of the hydration/dehydration reaction that occurs during ion exchange can be isolated.

The overall thermodynamic cycle that describes the cation exchange process coupled with the change in interlayer water content and structure is presented in Fig. 1.

2.2. Simulations

We recently developed a new *cis*-vacant molecular model for Wyoming-MMT, consistent with atomic-scale high-resolution transmission electron microscope imaging [30]. We showed that the interlayer water is more structurally-ordered with stronger hydrogen bonding in *cis*-vacant MMT than its commonly-used *trans*-vacant equivalent and the structure of the interlayer varies depending on the cations occupying it. Through grand canonical Monte Carlo (GCMC) simulations, we obtained the equilibrium basal spacing and water contents for stable hydration states of *cis*-vacant NaMMT and KMMT in a dilute suspension. We perform all our simulations on the *cis*-vacant molecular structure for MMT in this study. The clay unit cell parameters are $a = 5.20$ Å, $b = 9.00$ Å, $c = 10.07$ Å, $\alpha = \gamma = 90°$, and $\beta = 99.5°$. This unit cell is repeated in the a-b plane followed by isomorphic substitution of Mg^{2+} for Al^{3+} in the octahedral sheet resulting in a structural charge of $-0.57e$ per unit cell ($O_{20}(OH)_4$). It must be noted that the constraint of preventing two adjacent Mg^{2+} substitutions is not applicable to *cis*-vacant MMT. The simulations, carried out in LAMMPS [31], use ClayFF [32] to describe the van der Waals and electrostatic forces in the mineral and cations, and SPC/E for water [33]. Lennard-Jones interaction terms between dissimilar atom types are calculated via Lorentz-Berthelot mixing rules. We employ a cutoff distance of 15 Å for short-range interactions, and Ewald's summation method with an accuracy of 99.99% for long range electrostatics.

2.3. Swelling simulations

The energetics associated with the transition between hydration states requires the calculation of free energy changes through perturbations [34,35], alchemical transformations with thermodynamic integration (TI) [36], or reaction co-ordinate based simulations [37]. The calculation of the free energy difference between stable hydrates yields the swelling free energy at a given solution composition. Significant focus has been dedicated to the estimation of swelling free energies using molecular modeling [10,15,38–40] of *trans*-vacant MMT in dilute suspension. We employed the potential of mean force (PMF) approach in combination with umbrella sampling (along a pre-defined reaction co-ordinate), in a related study, to compute the swelling free energy of NaMMT as a function of ionic strength in homoionic solutions. As a result, the minima from the PMF profile yielded the equilibrium basal spacings and the relative probability for each hydration state as a function of bulk solution concentration. We also explored the likelihood of mixed hydration states existing in an interstratified microstructure within MMT tactoids [41].

Here, we simulate clay swelling in a series of aqueous solutions of variable concentration and composition. Simulations were performed in pure liquid water, in 1.0 M and 1.9 M NaCl solutions, and in 1.0 M KCl solution. Our molecular system consists of two parallel clay layers, made up of 175 unit cells each (9.35 nm × 9.05 nm), suspended in solution (see Fig. 2). The edges of clay layers perpendicular to the *x*-*z* plane were made unreactive with OH, OH_2 terminations that result in neutral edge charge. The system was equilibrated in the NPT ($T = 298$ K, $P = 1$ atm) ensemble for 1 ns, following which, a steered molecular dynamics (SMD) simulation was performed over 3 ns in the NP_zT ensemble. In the SMD run, the bottom MMT layer was tethered while the top MMT layer was translated along the *z*-direction with a constant velocity of 2 Å/ns by a harmonic stiff spring [42]. Subsequently, we segmented the entire SMD run into trajectory windows of 1 Å change in basal spacing and used the initial step of each window as input to perform umbrella sampling. The umbrella sampling, which was implemented using the Collective Variables (COLVARS) library in LAMMPS [43], spanned 40 stages per window, and each stage sampled the distance between the layers and the harmonic potential of the spring for a translation of 0.025 Å. The small size of umbrella windows ensured that there was sufficient sampling of the entire reaction co-ordinate (here, the reaction co-ordinate is the basal spacing) and overlap among the umbrella windows. Since the umbrella sampling approach imposes a biasing potential (here, the biasing potential is the harmonic potential of the stiff spring), we need an unbiasing algorithm to compute the PMF. We used the Weighted Histogram Analysis Method (WHAM) code [44] to extract the PMF profile from the umbrella sampling results. Ho et al. showed that the ClayFF parameter set does not predict the dry to one-water layer (0–1 W) hydration process well [9]. The authors of the study modified ClayFF to capture the dry to hydrated state transition. Since we used the traditional ClayFF parameters and because we are interested in the swelling states applicable to engineered barriers, our focus is restricted to the 2 W to 3 W transition.

2.4. Ion exchange simulations

The energetics associated with the replacement of ions in clay minerals has been studied over the last two decades using TI employed via molecular simulations [17,23,45]. However, as explained earlier, these studies assume a dilute aqueous phase, whereas we consider homoionic as well as mixed electrolyte solutions at higher ionic strength. The TI calculations are performed separately in the solution phase and the solid phase. In the solution phase, we start with homoionic 1.0 M NaCl and progressively transform 25% of Na^+ ions transformed into K^+ ions by changing their pairwise Lennard-Jones interaction parameters (i.e. σ for the distance of zero intermolecular potential and ε for the potential well depth) in a series of 11 steps, using a coupling parameter $\lambda \in [0, 1]$, with 0 representing Na^+, and 1 representing K^+, using equations given by:

$$\sigma(\lambda) = \sigma_{Na} + \lambda(\sigma_{Na} - \sigma_K) \tag{13a}$$

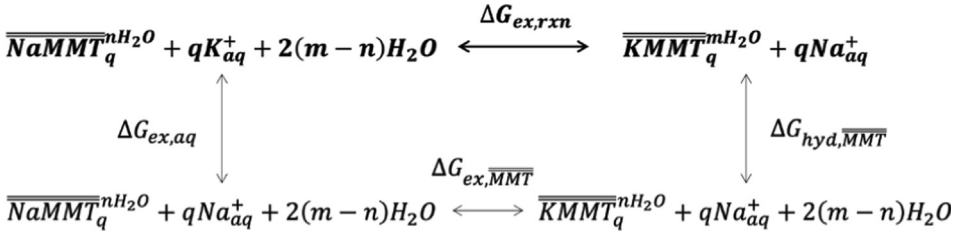

Fig. 1. Thermodynamic cycle for cation exchange coupled with change in equilibrium hydration content.

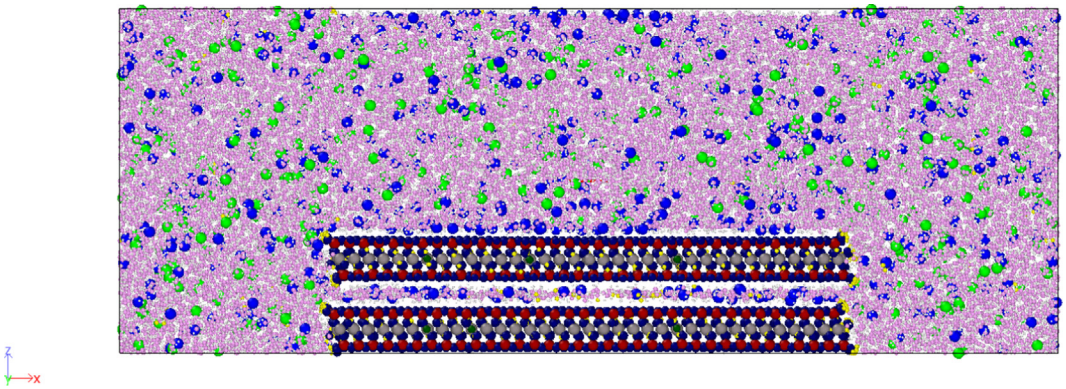

Fig. 2. System set-up for PMF simulations with umbrella sampling. The top mineral layer is translated away parallel to the bottom layer, which is fixed along *x* and *z*. The atoms along the *x*-*z* edges of the clay layers are terminated for neutral edge charge; the clay layer is infinitely large along the *y* direction. The atom color scheme is as follows: Al – grey, Mg – dark green, Si – dark red, O – navy blue, H atoms in clay layer – yellow, Na – blue, Cl – green, water O – pink, water H – white.

$$\varepsilon(\lambda) = \varepsilon_{Na} + \lambda(\varepsilon_{Na} - \varepsilon_K) \tag{13b}$$

At each step, an NPT equilibration for 3 ns follows the change in the Lennard-Jones interaction parameters. The result at the end of the transformation yields a mixed electrolyte solution containing 0.75 M NaCl and 0.25 M KCl. This series of progressive transformation steps are carried out until we arrive at solutions of 0.5 M, 0.75 M, and 1.0 M KCl (with progressively decreasing NaCl concentration). The variation in the Hamiltonian of the system during the transformation as a function of the coupling parameter λ allows the free energy calculation for the exchange reaction. The outcome of each series of TI simulations in the solution phase is the corresponding $\Delta G_{ex,aq}$term in Eq. (7).

$$\Delta G_{ex} = \int_{\lambda=0}^{\lambda=1} \langle \frac{\partial H}{\partial \lambda} \rangle d\lambda \tag{14}$$

We perform a similar series of TI simulations in the 2 W clay phase, starting with a volume containing 4 mineral layers (see Fig. 3) containing 24 unit cells of MMT each, with equilibrium basal spacings and water contents determined from the swelling simulations in the previous section. The MMT layers in this simulation are periodically replicated in *x*, *y*, and *z* directions and are therefore, infinitely large without terminated edges. The system is equilibrated (NPT) initially, followed by 3 ns of NP_zT equilibration with the modified force field potentials. The clay layers are rigid during the TI transformation, keeping the basal spacings fixed.

To understand the influence of tactoid composition on the free energy of the exchange reaction, we simulate partial ion exchange in an interstratified clay tactoid. Unlike homostructured clay where ion compositions are roughly equivalent in every interlayer, we simulate complete exchange in discrete layers, varying the total number of interlayers exchanged. For example, a 25% partial ion exchange corresponds to one out of the four interlayers being exchanged for K^+ (Fig. 3a). The individual interlayers consist of homogeneous cations and the choice of this methodology is supported by experimental data suggesting that interlayers contain unique cations during partial ion exchange [16,18]. Importantly, the water content is fixed during the TI calculations, so these simulation results can be used to isolate the effect of composition from that of basal spacing on the exchange free energy.

To separately determine the influence of local tactoid basal spacing/water content on the exchange reaction free energies, the ion exchange simulations in the clay phase are performed at three different equilibrium water contents for the 2 W state: 9.6 H_2O/uc, 10.2 H_2O/uc, and 11 H_2O/uc. These values correspond to the equilibrium water contents for 2 W KMMT, 2 W NaMMT, fully saturated 2 W MMT, respectively. From these TI simulations, we calculate the term $\Delta G_{\bar{ex,MMT}}$ in Equation (7) for both partial and complete ion exchange. Furthermore, we also compute the term $\Delta G_{\bar{hyd,MMT}}$ as a function of the deviation in water content based on Equation (12).

3. Results

The swelling free energy profiles from the PMF simulations of two parallel clay mineral layers suspended in aqueous solutions are presented in Fig. 4. The profiles yield the equilibrium basal spacings, equilibrium water contents for each stable hydrate/layer state, free energy changes due to deviations in water content for a fixed swelling state (e.g., $\Delta G_{\bar{hyd,MMT}}$ in Eq. (7)), and the energy to transition between states at a constant water and ion activity. The suspension of the clay particle in bulk water yields equilibrium 2 W (d_{001} = 15.8 Å), 3 W (d_{001} = 18.7Å), and 4 W (d_{001} = 21Å) crystalline swelling states with accessible free energy minima before the osmotic swelling regime begins (Fig. 4). The 3 W hydration state is, however, the most favored swelling state with the lowest free energy containing approximately 15 H_2O/uc (Fig. 4a). As the solution concentration in which the clay particle is saturated increases, the preference shifts towards lower swelling states (2 W) and the free energy difference to access the higher swelling state increases, i.e., $\Delta G_{3W-2W,1.9MNaCl} > \Delta G_{3W-2W,1.0MNaCl}$. We also observe only a shallow potential well associated with the 4 W hydration state for the clay particle in the 1.0 M and 1.9 M solutions and the minima are not statistically significant based on the error estimates. These profiles indicate that clay compaction is favored in the presence of concentrated solutions, which has been supported by recent experimental and computational studies [17,46,47], and that the degree of compaction depends on the solution chemistry.

Changes in chemical composition and concentration are also shown to exert a significant influence on the equilibrium basal spacing (and therefore, the equilibrium water content since the interlayer cation does not vary) of the stable hydrates. The equilibrium basal spacings in 1.0 M solution for the 2 W and 3 W KMMT layers are 15.9 Å and 18.9 Å respectively, whereas the 2 W and 3 W basal spacings for the NaMMT layers are 16.05 Å and 18.8 Å, respectively. The equilibrium water contents for the 2 W state are 9.6 H_2O/uc and 10.2 H_2O/uc for KMMT and NaMMT, respectively. The free energy impact of small deviations in basal spacing (water content) around the free energy minima also varies with solution conditions. Steeper potential wells generate larger energy perturbations for the same change in water content, giving larger

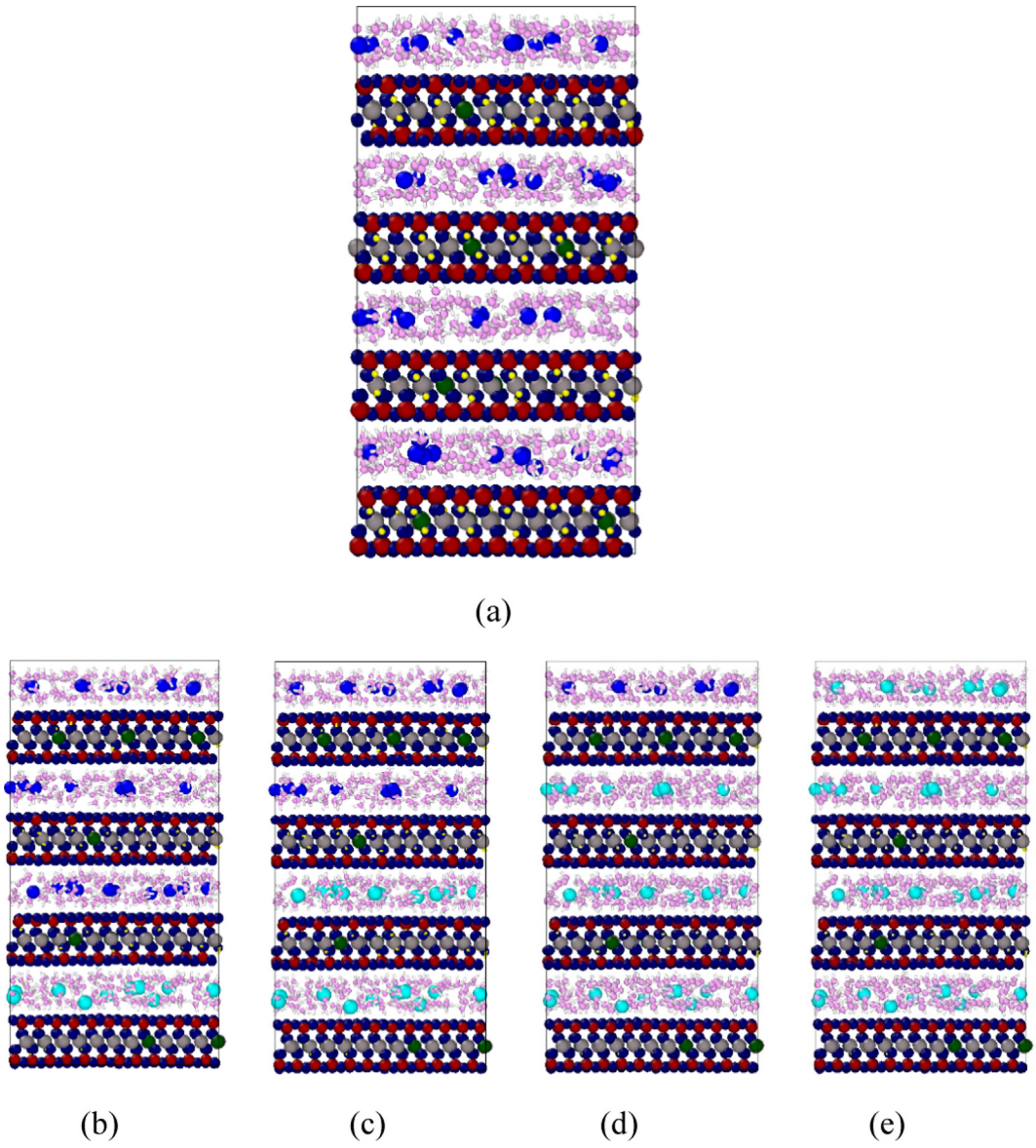

Fig. 3. (a) System set up for clay-phase TI simulations. The initial basal spacings are determined based on the 2 W minima from the swelling simulations. Na^+ ions are alchemically transformed to K^+ ions in a series of 11 steps. (b) 25% exchange of Na^+ ions to K^+ ions; (c) 50% exchange; (d) 75% exchange; (e) 100% exchange. The atom color scheme is as follows: Al – grey, Mg – dark green, Si – dark red, O – navy blue, H atoms in clay layer – yellow, Na – blue, K – cyan, water O – pink, water H – white.

values of $\Delta G_{hyd.MMT}$ (Eq. (7)). A 2 W hydrate is favorable in both cases (NaMMT and KMMT) when suspended in 1.0 M solution, and the swelling free energy differences between the 2 W and 3 W states are similar at ~ 5.5 kJ/mol of clay. However, the slopes leading up to the 2 W minima are opposite in magnitude for the two systems, indicating that there may be a more favorable minimum corresponding to a 1 W state for KMMT at this water/ion activity. In the case of the NaMMT system, the 2 W state appears to be the global minimum and the higher crystalline and osmotic states are accessible within 12 kJ/mol. The 2 W states for both 1.0 M NaCl and KCl are both associated with relatively shallow potential wells, and deviations in the basal spacing associated with a change in composition from NaMMT to KMMT (0.15 Å) is less than 0.5 kJ/mol for both end-members.

The free energies of isovalent ion exchange in aqueous solution as a function of solution composition (at fixed concentration) are presented in Fig. 5. In the past, the free energy of ion exchange in aqueous solution has been computed as the difference in the ion hydration energies assuming a dilute solution. Based on this computation, the exchange free energy of $Na^+ \rightarrow K^+$ in solution is found to be 72 – 84 kJ/mol [28,48]. The exchange of the free energy computed with Smith-Dang parameterizations for the monovalent ions in an SPC/E water model yields 89 kJ/mol [49,50]. However, we observe a strong concentration dependence on this value implying that the exchange of K^+ for Na^+ is more favorable in concentrated solutions. This could be because the hydration shells of ions in 1.0 M solution are partially complete and contain fewer water molecules per ion to shed as they undergo exchange. We also observe a small composition dependence from the data in Fig. 5. The aqueous exchange of $K^+ \rightarrow Na^+$ in solution (which in turn, drives the formation of KMMT) is more favorable in a mixed electrolyte with a higher mole fraction of K^+ to begin with. Therefore, potassium-rich mixed electrolytes exhibit a stronger drive for exchange reactions in MMT, because the solution has a greater tendency to accept Na^+ ions.

Data from our TI simulations in the solid and aqueous phases are combined to obtain the overall free energy of the exchange

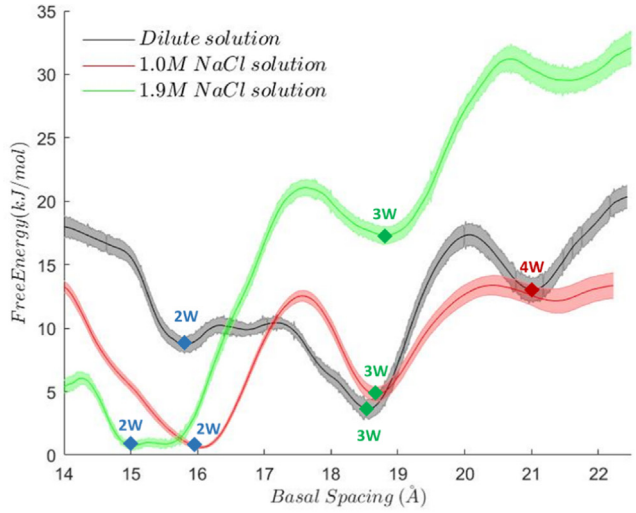

(a)

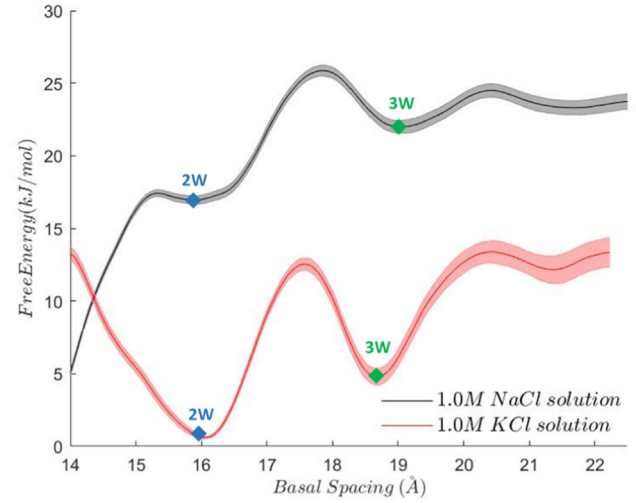

(b)

Fig. 4. Potential of mean force (PMF) profile as a function basal spacing (d_{001} which was defined as the reaction co-ordinate) between MMT layers (a) suspended in bulk water and NaCl solutions of different concentrations; (b) suspended in 1.0 M aqueous solutions with different cations. Results indicate the equilibrium basal spacings for the 2 W and 3 W state in the respective solution conditions and the difference in their free energies.

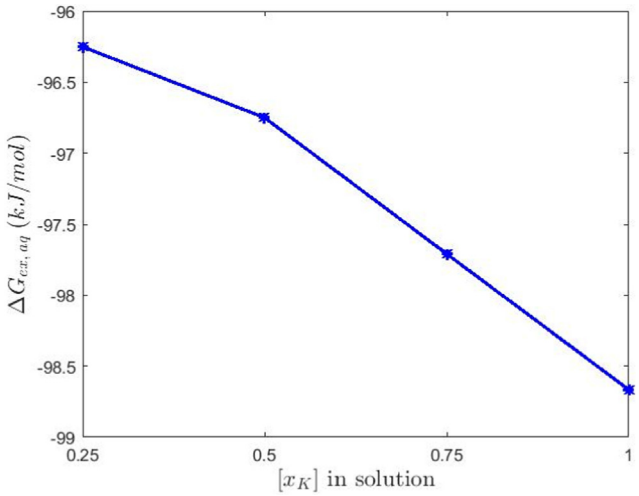

Fig. 5. Free energy of ion exchange ($K^+ \rightarrow Na^+$) in aqueous solution of total ionic strength of 1.0 M. The plot shows a dependence of the free energy of ion exchange on the equilibrium composition of the mixed electrolyte solution at a fixed concentration.

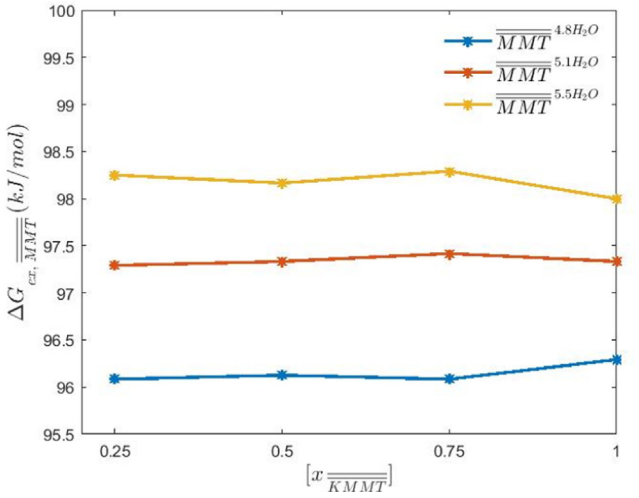

Fig. 6. Free energy of ion exchange ($Na^+ \rightarrow K^+$) as a function of the extent of the exchange reaction (partial to complete exchange) in a clay platelet containing different equilibrium water contents. The data shows that the equilibrium water content in the clay interlayer exerts a larger influence on the exchange free energy than the composition of the clay phase ($x_{\overline{KMMT}}/x_{\overline{NaMMT}}$).

reaction. Fig. 6 illustrates this information as a function of solution composition for different equilibrium water contents over a range of solid compositions. Surprisingly, the exchange reaction free energy is independent of the solid composition for interstratified clays with uniform water content/basal spacing. The reaction constants for the overall exchange reaction are plotted against the mole fraction of K^+ in solution (composition of mixed electrolyte) for each degree of ion exchange (ranging from partial to complete ion exchange) in the clay phase in Fig. 7. These results demonstrate that the stability constant for the exchange reaction in Eq. (3) ($K_{c,rxn}$) increases exponentially with increasing KCl fraction in solution. This implies that the solution phase, initially consisting of a high fraction of K^+ ions, is more readily accepting of Na^+ ions from the solid phase, consistent with our findings in Fig. 5. The exchange of K^+ for Na^+ (both partial and complete) favors the interlayer with a lower water content, explaining the higher selectivity of interlayers with a lower water content (at a fixed hydration state) for potassium over sodium ions. To elaborate this further, we illustrate the free energy for the overall exchange reaction in different mixed electrolytes in Fig. 8. When $\overline{NaMMT}$ is suspended in 1.0 M KCl solution, the exchange reaction – both partial and complete – is favorable across all three equilibrium water contents. However, as we consider mixed electrolyte solutions that are rich in sodium, the exchange reaction of $\overline{NaMMT}$ to $\overline{KMMT}$ is feasible only for $m = 4.8$, and a complete exchange is barely favorable. Interlayers with a higher water content do not undergo exchange spontaneously. The data exhibits a strong sensitivity to the composition of the solution and the equilibrium interlayer water content, but not to the degree of exchange in neighboring layers, i.e., the exchange selectivity is almost unaffected by the solid phase composition in our simulations.

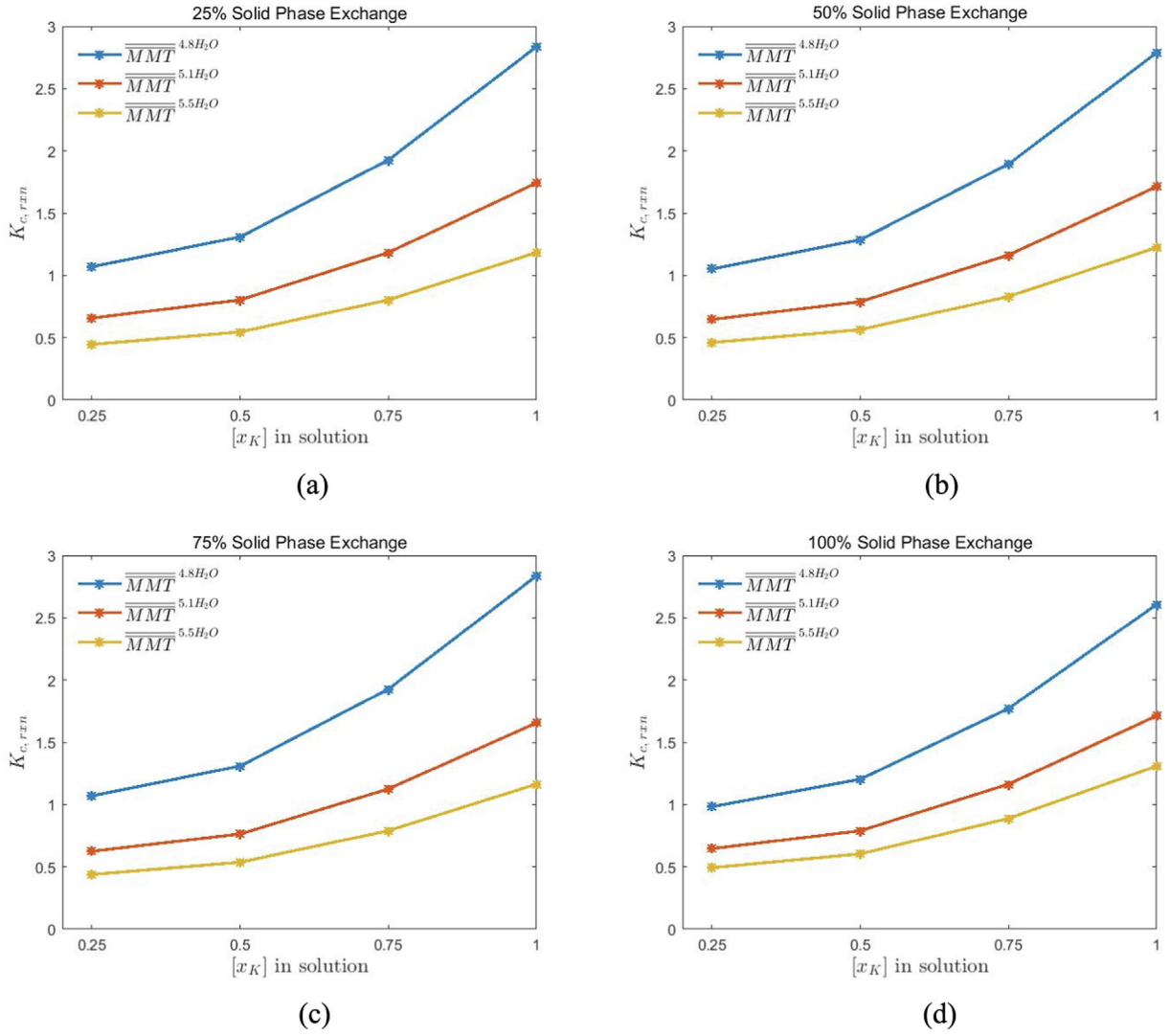

Fig. 7. Equilibrium constants for the overall ion exchange reaction as a function of solution composition and different degrees of exchange. (a) 25% ion exchange in clay platelet with interlayers consisting of unique cations; (b) 50% ion exchange; (c) 75% ion exchange; (d) complete ion exchange in clay platelet.

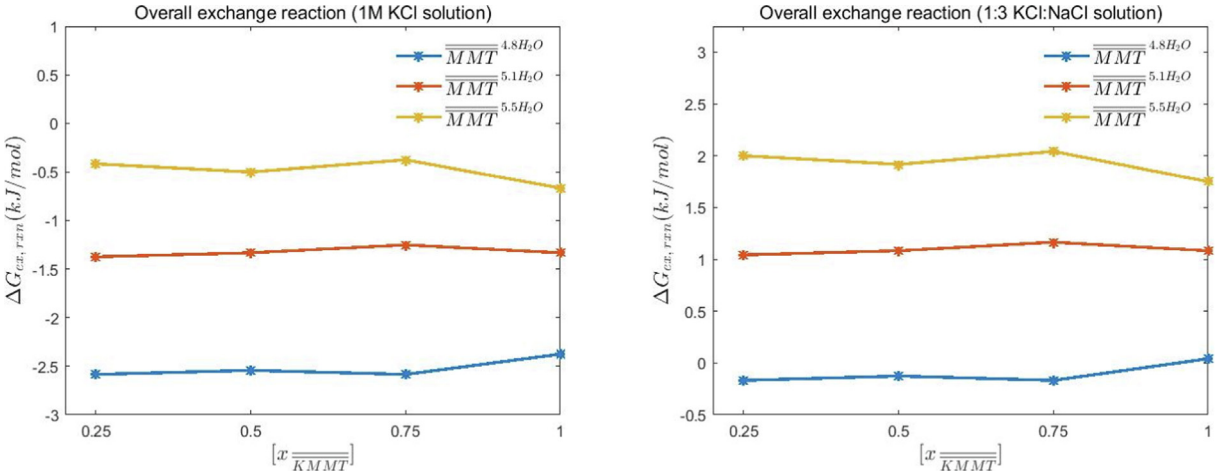

Fig. 8. Gibbs free energy for the ion exchange reaction as a function of degree/extent of exchange at various mixed electrolyte compositions. (a) 1.0 M KCl aqueous solution; (b) mixed electrolyte with 0.25KCl + 0.75 M NaCl.

4. Discussion

The exchange of isovalent ions in clay minerals is tightly coupled with a change in water content in the interlayers, which occurs from an overall change in the swelling state or a change in the hydration structure at a constant swelling state. The swelling and ion exchange reactions simulated in this study enable us to understand the influence of solution chemistry (concentration and composition) and solid composition on the coupled processes. The TI simulations in the aqueous phase yield the free energy of cation exchange in a solution of given composition. Using these free energy values ($\Delta G_{ex,aq}$) in the aqueous phase to compute the chemical potentials/activity coefficients of the ions in solution using Eq. (8) allows us to relax the assumption of equal activity coefficients for isovalent ions. Furthermore, we find that the $\Delta G_{ex,aq}$ is not equal to the difference in hydration energies of Na^+ and K^+ ions in dilute solution. There is a concentration dependence ($\Delta G_{ex,\infty}$ 80 kJ mol^{-1}, $\Delta G_{ex,1Maq}$ 97 kJ mol^{-1})and a small composition dependence ($\pm$2 kJ mol^{-1}) for the aqueous exchange free energy.

The equilibrium constants of the overall ion exchange reactions expressed as a function of ion activities (a_{Na}/a_K) and the interlayer water content indicate that the equilibrium composition ($x_{\bar{KMMT}}, x_{\bar{NaMMT}}$) of the solid clay phase plays an insignificant role in our simulations. The equilibrium water content, however, is an important factor for the spontaneity of ion exchange ($Na^+ \rightarrow K^+$) in the solid phase. At clay interlayers with a high equilibrium water content *n = 5.1 or 5.5,* for example, exchange favorability in the solid phase significantly reduces in the presence of mixed electrolytes. Furthermore, the mineral does not exhibit any selectivity to the exchange when a_{Na}/a_K is high. This supports why poorly hydrated clay is more selective to K^+ whereas saturated clay is more selective to Na^+ even while not being accompanied with a change in the swelling state. Thus, the results in Figs. 6 and 7 strongly highlight the influence of interlayer solvation structure on driving exchange favorability for a given water and aqueous ion activity.

We also observe a strong dependence on the solution composition for the ion exchange reaction. At a given concentration, the ratio of ion activities (composition of the mixed electrolyte) appears to drive the exchange selectivity, particularly for equilibrium water contents. In the case of $\bar{MMT}^{5.1H_2O}$, the overall exchange reaction is favorable only when the aqueous solution is rich in K^+ whereas for $\bar{MMT}^{5.5H_2O}$, spontaneous ion exchange occurs only in the case of pure KCl solution.

The solid phase composition exerts very little influence on the ion exchange reaction free energy here, likely because the clay particle simulations here involve rigid clay layers with fixed water contents. This finding underscores the much greater importance of structural water content and basal spacing for chemo-mechanically coupled ion exchange reactions in swelling clays. Evidence in literature points to the favorable occurrence of tactoid phase separation (e.g., homostructured tactoids populated with unique cations). Whittaker et al. [18] showed this to be the case at low- to mid-range a_{Na}/a_K. The study also confirmed the presence of coexisting populations of phase-separated clay tactoids based on their hydration state, although no conclusion could be drawn on phase separation based on cation type. Our simulations model partial ion exchange resulting in interstratified interlayers with unique cations in an interlayer. Relaxation and equilibration of the structure allowing for changes to the basal spacing and changes to the water content, perhaps with concurrent grand canonical Monte Carlo (GCMC) simulations, could help to directly quantify the influence of solid phase composition on the ion exchange reaction due to variable cation hydration in the interlayer. However, designing a closed thermodynamic cycle to perform TI simulations can be challenging with this added degree of freedom. The extracted stress data from the interlayers in our NPT simulations confirms the tendency of the interlayers to relax their basal spacings as the degree of exchange progresses (as the solid phase has a greater $x_{\bar{KMMT}}$ composition). For example, we observe greater compressive stresses in the clay particle when the solid phase is $\bar{KMMT}$-rich ($x_{\bar{KMMT}} > 0.5$). The magnitudes of compressive stresses also increase with an increase in the equilibrium water content, i.e., $\bar{KMMT}^{5.5H_2O}$ interlayers exhibit a stronger tendency to collapse subsequent to partial and/or ion exchange than $\bar{KMMT}^{4.8H_2O}$.

5. Conclusions

We model the swelling and ion exchange reactions in a swelling clay mineral (MMT) and compute the free energies of the reactions using PMF and TI based molecular simulations, respectively, for the 2 W swelling state. The free energies of phase transformation and ion exchange are used to compute the selectivities of hydration states for cations. Studies that usually model ion exchange do not account generally for varying water contents (from changes to the equilibrium swelling state and the equilibrium water content for the same swelling state) [22,23], whereas our ion exchange simulations yield the exchange reaction free energies as a function of both the clay composition and the change in interlayer water content. We also consider the effect of aqueous electrolyte composition on the ion exchange energies. Instead of performing trace exchange via thermodynamic integration simulations as most studies in literature [17,22,23], we allow for ion-ion interactions in the aqueous phase. The free energy of ion exchange in aqueous solution, therefore, is not just the difference of the hydration enthalpies (in dilute suspension) of the exchanged ions in this case but varies based on the initial composition of the aqueous solution. The aqueous solution composition and clay water content are shown to exert a much greater influence on exchange reaction spontaneity than the clay composition. Thus, we conclude that the tendency for individual layers (and indeed whole tactoids) to segregate are driven by the extremely strong coupling between basal spacing (controlled by water content here) and free energy in the clay crystalline hydrates.

CRediT authorship contribution statement

Nithya Subramanian: Conceptualization, Methodology, Investigation, Formal analysis, Visualization, Writing– original draft, Writing – review & editing. **Laura Nielsen Lammers:** Methodology, Formal analysis, Writing – review & editing, Supervision.

Declaration of Competing Interest

The authors declare that they have no known competing financial interests or personal relationships that could have appeared to influence the work reported in this paper.

Acknowledgement

This work was supported by the U.S. Department of Energy Nuclear Energy program, Engineered Barrier Systems R & D (SF-19LB01030802). We thank Piotr Zarzycki for insight on the reaction co-ordinates and setting up thermodynamic cycles for our molecular dynamic simulations. The MD simulations reported in

this paper were carried out using resources of the National Energy Research Scientific Computing Center (NERSC).

References

[1] T.T. Meetei, Y.B. Devi, T.T. Chanu, Ion Exchange: The Most Important Chemical Reaction on Earth after Photosynthesis, Int. Res. J. Pure Appl. Chem. 31–42 (2020), https://doi.org/10.9734/irjpac/2020/v21i630174.

[2] A. Hassanvand, K. Wei, S. Talebi, G. Chen, S. Kentish, The Role of Ion Exchange Membranes in Membrane Capacitive Deionisation, Membranes 7 (2017) 54, https://doi.org/10.3390/membranes7030054.

[3] S.G. Christensen, Thermodynamics of Aqueous Electrolyte Solutions - Application to Ion Exchange Systems, Department of Chemical Engineering, Technical University of Denmark, København, 2005.

[4] L. Wang, H. Sun, Prediction of Na^+ /NH_4^+ Exchange in Faujasite Zeolite by Molecular Dynamics Simulation and Thermodynamic Integration Method, J. Phys. Chem. C 117 (27) (2013) 14051–14060, https://doi.org/10.1021/jp403326n.

[5] P. Sellin, O.X. Leupin, The Use of Clay as an Engineered Barrier in Radioactive-Waste Management – A Review, Clays Clay Miner. 61 (2013) 477–498, https://doi.org/10.1346/CCMN.2013.0610601.

[6] K. NORRISH, Crystalline Swelling of Montmorillonite: Manner of Swelling of Montmorillonite, Nature 173 (4397) (1954) 256–257, https://doi.org/10.1038/173256a0.

[7] I.C. Bourg, G. Sposito, Molecular Dynamics Simulations of the Electrical Double Layer on Smectite Surfaces Contacting Concentrated Mixed Electrolyte (NaCl–CaCl2) Solutions, J. Colloid Interface Sci. 360 (2011) 701–715, https://doi.org/10.1016/j.jcis.2011.04.063.

[8] S.L. Teich-McGoldrick, J.A. Greathouse, C.F. Jové-Colón, R.T. Cygan, Swelling Properties of Montmorillonite and Beidellite Clay Minerals from Molecular Simulation: Comparison of Temperature, Interlayer Cation, and Charge Location Effects, J. Phys. Chem. C 119 (36) (2015) 20880–20891, https://doi.org/10.1021/acs.jpcc.5b03253.

[9] T.A. Ho, L.J. Criscenti, J.A. Greathouse, Revealing Transition States during the Hydration of Clay Minerals, J. Phys. Chem. Lett. 10 (2019) 3704–3709, https://doi.org/10.1021/acs.jpclett.9b01565.

[10] H.D. Whitley, D.E. Smith, Free Energy, Energy, and Entropy of Swelling in Cs–, Na–, and Sr–Montmorillonite Clays, J. Chem. Phys. 120 (2004) 5387–5395, https://doi.org/10.1063/1.1648013.

[11] F. Salles, J.-M. Douillard, O. Bildstein, C. Gaudin, B. Prelot, J. Zajac, H. Van Damme, Driving Force for the Hydration of the Swelling Clays: Case of Montmorillonites Saturated with Alkaline-Earth Cations, J. Colloid Interface Sci. 395 (2013) 269–276, https://doi.org/10.1016/j.jcis.2012.12.050.

[12] D. Laird, Relationship Between Cation Exchange Selectivity and Crystalline Swelling in Expanding 2:1 Phyllosilicates, Clays Clay Miner. 45 (1997) 681–689, https://doi.org/10.1346/CCMN.1997.0450507.

[13] L. Massat, O. Cuisinier, I. Bihannic, F. Claret, M. Pelletier, F. Masrouri, S. Gaboreau, Swelling Pressure Development and Inter-Aggregate Porosity Evolution upon Hydration of a Compacted Swelling Clay, Appl. Clay Sci. 124–125 (2016) 197–210, https://doi.org/10.1016/j.clay.2016.01.002.

[14] Y.-W. Hsiao, M. Hedström, Swelling Pressure in Systems with Na-Montmorillonite and Neutral Surfaces: A Molecular Dynamics Study, J. Phys. Chem. C 121 (47) (2017) 26414–26423, https://doi.org/10.1021/acs.jpcc.7b09496.

[15] T. Honorio, L. Brochard, M. Vandamme, Hydration Phase Diagram of Clay Particles from Molecular Simulations, Langmuir 33 (44) (2017) 12766–12776, https://doi.org/10.1021/acs.langmuir.7b03198.

[16] Y.W. Li, C.P. Schulthess, Ion-exchange modeling of monovalent alkali cation adsorption on montmorillonite, Clays Clay Miner. 68 (2020) 476–490, https://doi.org/10.1007/s42860-020-00091-9.

[17] H. Zhou, M. Chen, R. Zhu, X. Lu, J. Zhu, H. He, Coupling between Clay Swelling/Collapse and Cationic Partition, Geochim. Cosmochim. Acta 285 (2020) 78–99, https://doi.org/10.1016/j.gca.2020.07.007.

[18] M.L. Whittaker, L.N. Lammers, S. Carrero, B. Gilbert, J.F. Banfield, Ion exchange selectivity in clay is controlled by nanoscale chemical-mechanical coupling, Proc. Natl. Acad. Sci. 116 (2019) 22052–22057, https://doi.org/10.1073/pnas.1908086116.

[19] H. Jenny, Simple kinetic theory of ionic exchange. I. Ions of equal valency, J. Phys. Chem. 40 (1936) 501–517.

[20] G.H. Bolt, Ion adsorption by clays, Soil Sci. 79 (1955) 267–276.

[21] I. Shainberg, Charge density and Na-K-Ca exchange on smectites1, Clays Clay Miner. 35 (1987) 68–73, https://doi.org/10.1346/CCMN.1987.0350109.

[22] B.J. Teppen, D.M. Miller, Hydration energy determines isovalent cation exchange selectivity by clay minerals, Soil Sci. Soc. Am. J. 70 (2006) 31–40, https://doi.org/10.2136/sssaj2004.0212.

[23] B. Rotenberg, J.-P. Morel, V. Marry, P. Turq, N. Morel-Desrosiers, On the driving force of cation exchange in clays: insights from combined microcalorimetry experiments and molecular simulation, Geochim. Cosmochim. Acta 73 (14) (2009) 4034–4044, https://doi.org/10.1016/j.gca.2009.04.012.

[24] C. Tournassat, H. Gailhanou, C. Crouzet, G. Braibant, A. Gautier, E.C. Gaucher, Cation exchange selectivity coefficient values on smectite and mixed-layer illite/smectite minerals, Soil Sci. Soc. Am. J. 73 (2009) 928–942, https://doi.org/10.2136/sssaj2008.0285.

[25] T. Missana, A. Benedicto, M. García-Gutiérrez, U. Alonso, Modeling cesium retention onto Na-, K- and Ca-smectite: effects of ionic strength, exchange and competing cations on the determination of selectivity coefficients, Geochim. Cosmochim. Acta 128 (2014) 266–277, https://doi.org/10.1016/j.gca.2013.10.007.

[26] B. Baeyens, M.H. Bradbury, Cation exchange capacity measurements on illite using the sodium and cesium isotope dilution technique: effects of the index cation, electrolyte concentration and competition: modeling, Clays Clay Miner. 52 (2004) 421–431, https://doi.org/10.1346/CCMN.2004.0520403.

[27] V.N. Afanasiev, A.N. Ustinov, I.Y. Vashurina, State of hydration shells of sodium chloride in aqueous solutions in a wide concentration range at 273.15−373.15 K, J. Phys. Chem. B 113 (1) (2009) 212–223, https://doi.org/10.1021/jp711542j.

[28] Y. Marcus, Concentration dependence of ionic hydration numbers, J. Phys. Chem. B 118 (35) (2014) 10471–10476, https://doi.org/10.1021/jp5039255.

[29] J. Teychené, H.R. Balmann, L. Maron, S. Galier, Investigation of ions hydration using molecular modeling, J. Mol. Liq. 294 (2019), https://doi.org/10.1016/j.molliq.2019.111394 111394.

[30] N. Subramanian, M.L. Whittaker, C. Ophus, L.N. Lammers, Structural implications of interfacial hydrogen bonding in hydrated wyoming-montmorillonite clay, J. Phys. Chem. C 124 (16) (2020) 8697–8705, https://doi.org/10.1021/acs.jpcc.9b1133910.1021/acs.jpcc.9b11339.s00110.1021/acs.jpcc.9b11339.s002.

[31] S. Plimpton, A. Kohlmeyer, A. Thompson, S. Moore, R. Berger, LAMMPS Stable Release 29 October 2020; Zenodo, 2020.

[32] R.T. Cygan, J.-J. Liang, A.G. Kalinichev, Molecular models of hydroxide, oxyhydroxide, and clay phases and the development of a general force field, J. Phys. Chem. B 108 (4) (2004) 1255–1266, https://doi.org/10.1021/jp0363287.

[33] B. Pullman, Intermolecular Forces: Proceedings of the Fourteenth Jerusalem Symposium on Quantum Chemistry and Biochemistry Held in Jerusalem, Israel, April 13-16, 1981, Springer Netherlands: Dordrecht, 2010; ISBN 978-94-015-7658-1.

[34] L.D. Landau, E.M. Lifshitz, L.P. Pitaevskii, J.B. Sykes, M.J. Kearsley, Statistical Physics. Volume 5 of Course of Theoretical Physics. Part 1 Volume 5 of Course of Theoretical Physics, Part 1; 1980; ISBN 978-1-4831-0337-2.

[35] C.H. Bennett, Efficient Estimation of Free Energy Differences from Monte Carlo Data, J. Comput. Phys. 22 (1976) 245–268, https://doi.org/10.1016/0021-9991(76)90078-4.

[36] M. Zacharias, T.P. Straatsma, J.A. McCammon, Separation-shifted scaling, a new scaling method for Lennard-Jones interactions in thermodynamic integration, J. Chem. Phys. 100 (1994) 9025–9031, https://doi.org/10.1063/1.466707.

[37] C. Jarzynski, Nonequilibrium equality for free energy differences, Phys. Rev. Lett. 78 (1997) 2690–2693, https://doi.org/10.1103/PhysRevLett.78.2690.

[38] D.E. Smith, Y.u. Wang, A. Chaturvedi, H.D. Whitley, Molecular simulations of the pressure, temperature, and chemical potential dependencies of clay swelling †, J. Phys. Chem. B 110 (40) (2006) 20046–20054, https://doi.org/10.1021/jp062235o.

[39] M. Svoboda, F. Moučka, M. Lísal, Saturated Aqueous NaCl Solution and Pure Water in Na-Montmorillonite Clay at Thermodynamic Conditions of Hydraulic Fracturing: Thermodynamics, Structure and Diffusion from Molecular Simulations, J. Mol. Liq. 271 (2018) 490–500, https://doi.org/10.1016/j.molliq.2018.08.144.

[40] T.R. Underwood, I.C. Bourg, Large-Scale Molecular Dynamics Simulation of the Dehydration of a Suspension of Smectite Clay Nanoparticles, J. Phys. Chem. C 124 (6) (2020) 3702–3714, https://doi.org/10.1021/acs.jpcc.9b1119710.1021/acs.jpcc.9b11197.s00110.1021/acs.jpcc.9b11197.s002.

[41] L. Zheng, L. Lammers, P. Fox, Chun Chang, Hao Xu, Borglin Sharon, Michael Whittaker, Cunwei Chou, C. Tournassat, N. Subramanian, et al., Engineered Barrier System Research Activities at LBNL: FY20 Progress Report; 2020; p. LBNL-2001331, 1642698, ark:/13030/qt5hr7k5n1;

[42] S. Park, K. Schulten, Calculating potentials of mean force from steered molecular dynamics simulations, J. Chem. Phys. 120 (2004) 5946–5961, https://doi.org/10.1063/1.1651473.

[43] G. Fiorin, M.L. Klein, J. Hénin, Using collective variables to drive molecular dynamics simulations, Mol. Phys. 111 (2013) 3345–3362, https://doi.org/10.1080/00268976.2013.813594.

[44] A. Grossfield, WHAM: The Weighted Histogram Analysis Method.

[45] L.N. Lammers, I.C. Bourg, M. Okumura, K. Kolluri, G. Sposito, M. Machida, Molecular dynamics simulations of cesium adsorption on illite nanoparticles, J. Colloid Interface Sci. 490 (2017) 608–620, https://doi.org/10.1016/j.jcis.2016.11.084.

[46] X. Shen, I.C. Bourg, Molecular dynamics simulations of the colloidal interaction between smectite clay nanoparticles in liquid water, J. Colloid Interface Sci. 584 (2021) 610–621, https://doi.org/10.1016/j.jcis.2020.10.029.

[47] N.C.M. Marty, S. Grangeon, A. Lassin, B. Madé, P. Blanc, B. Lanson, A quantitative and mechanistic model for the coupling between chemistry and clay hydration, Geochim. Cosmochim. Acta 283 (2020) 124–135, https://doi.org/10.1016/j.gca.2020.05.029.

[48] L.H. Pettit, Metal ions in solution, Biochem. Educ. 7 (1979) 24, https://doi.org/10.1016/0307-4412(79)90032-3.

[49] I.S. Joung, T.E. Cheatham, Determination of alkali and halide monovalent ion parameters for use in explicitly solvated biomolecular simulations, J. Phys. Chem. B 112 (30) (2008) 9020–9041, https://doi.org/10.1021/jp8001614.

[50] I.S. Joung, T.E. Cheatham, Molecular dynamics simulations of the dynamic and energetic properties of alkali and halide ions using water-model-specific ion parameters, J. Phys. Chem. B 113 (40) (2009) 13279–13290, https://doi.org/10.1021/jp902584c.